Cell. Mol. Biol. (ISSN: 1165-158X)

Journal Homepage: www.cellmolbiol.org

Cellular and Molecular Biology

Original Article

MiR-146a alleviates acute lung injury via inhibiting Notch 1 signaling pathway targeting macrophage

Qiumin Zhao[1,#], Yan Wang[1,#], Jing Zou[2], Rong Kuang[3], Shiyan Ji[4,*]

[1] *Department of Clinical Laboratory, Changzhou Children's Hospital of Nantong University, Changzhou, China*
[2] *Department of Pneumology, Changzhou Children's Hospital of Nantong University, Changzhou, China*
[3] *Department of Anesthesiology, Changzhou Children's Hospital of Nantong University, Changzhou, China*
[4] *Children's Health Research Center, Changzhou Children's Hospital of Nantong University, Changzhou, China*

Article Info

Article history:

Received: November 12, 2023
Accepted: January 12, 2023
Published: January 31, 2024

Use your device to scan and read the article online

Abstract

Acute lung injury (ALI) is associated with leukocyte infiltration and inflammation. Previous studies have shown that miR-146a is a valid regulator of the macrophage polarization in vitro inflammatory model. However, it is unclear whether miR-146a plays a protective role in ALI via modulating macrophage inflammation. To explore the potential therapeutic effect mechanism of miR-146a on ALI. We analyzed the expression of miR-146a in acutely injured lung tissues and differentiated macrophages. Lipopolysaccharide (LPS) and interleukin-4 (IL-4) were employed in provoking the macrophage polarization. We used miR-146a mimics to improve the overexpression of miR-146a and investigated the effect of increased miR-146a on LPS-induced ALI mice via the target of macrophage polarization. We showed that the expression of miR-146a markedly decreased in injured lung tissue and type M1 macrophage, while increased miR-146a expression exhibited in type M2 macrophage. Moreover, overexpression of miR-146a in LPS-induced macrophage reversed inflammatory M1 phenotype to anti-inflammatory M2 phenotype and mitigated inflammatory level via inhibiting Notch 1 signaling pathway. Hence, inflammation, infiltration, integrity of capillary barrier, and histology in ALI model were corrected after miR-146a overexpression treatment. These results suggested that miR-146a promotes type M2 macrophage polarization via restraining Notch 1 signaling pathway. Overexpression of miR-146a prevents inflammation damage and ameliorates lung damage after LPS induction. Therefore, miR-146a may serve as a promising target for the therapy of ALI in the future.

Keywords: MiR-146a, Macrophage polarization, Acute lung injury, Notch 1 signaling pathway.

1. Introduction

Acute respiratory distress syndrome (ARDS) is one of the intractable clinical diseases in the Department of Critical Care Medicine [1,2]. Acute lung injuries associated with ARDS are stimulated by multiple pathogenic cytokines that lead to a large number of inflammation and necrosis of alveoli, which can engender hypoxemia, respiratory failure, and even death [3]. Many etiologies are inducing ALI, such as pneumonia, aspiration, pulmonary contusion, and multiple trauma [4,5]. Exploring effective lung protection therapy in the early stage has always been the goal of current research. Lung injury involves many pathological progressions, including immune response, inflammatory response, oxidative stress, necrosis and apoptosis [6-8]. When ALI occurs, the intrinsic immune system, such as macrophages, NK cells, and neutrophils can be first activated by the breakdown products of damaged lung cells and exogenous antigens. Then, adaptive immune response activation including effector T cells and B cells exerts corresponding effects.

Increasing studies [9-11] have reported that the expression of various genes plays a critical role after ALI. MicroRNA (miRNA) has been proven to be an important post-transcriptional regulatory target owing to its inhibition of mRNA translation [12]. MiRNA, discovered in Caenorhabditis elegans, is endogenous and short non-coding RNA [13]. In humans and other animals, miRNAs mainly get through binding with the 3' untranslated region (3' UTR) of target mRNAs to modulate the expression of target mRNAs or inhibit their translation procedure, which interferes with post-transcriptional gene expression and regulate the function in cells [14]. It is a universal gene regulation mode in cell bioactivity. Moreover, many miRNAs jointly regulate the same gene [15], hence, it is feasible that miRNAs have a coefficient effect on the post-transcriptional regulation of multifarious gene expression. Feng et al. [16] demonstrated that Ly6G+ neutrophil-derived miR-223 inhibits the NLRP3 inflammasome in mitochondrial DAMP-induced ALI, and Ying et al. [17] reported NLRP3 inflammasome activation by miR-495 in the progression of acute lung injury. However, the miR-146a effect on ALI is still elusive. In the study, we sought the

* Corresponding author.
E-mail address: Shiyanji1206@163.com (Shiyan Ji).
# These authors contributed equally
Doi: http://dx.doi.org/10.14715/cmb/2024.70.1.5

role of miR-146a in ALI, and by LPS-induced inflammation macrophage model and murine ALI model, we probed whether miR-146a overexpression administration affected macrophage phenotype and ALI improvement. Based on these obtained outcomes, miR-146a overexpression treatment exerts the anti-inflammation in macrophages and the potential therapy for ALI.

2. Materials and methods

2.1. Cells culture and treatment

RAW 267.4 macrophage line was purchased from American Type Culture Collection (ATCC) (Manassas, VA, USA) and cultured in Dulbecco's Modified Eagle's Medium medium (DMEM, KeyGEN, Nanjing, China) supplemented 10% fetal bovine serum (FBS; Gibco, Rockville, MD, USA) and 1% penicillin/streptomycin. RAW 267.4 was seeded in 5×5 cm_2 flask, and induced type M1 differentiation or type M2 differentiation using LPS (100 ng/mL, Sigma, St. Louis, MO, USA) or IL-4 (20 ng/mL, Sigma, St. Louis, MO, USA) for 24 h.

2.2. Transfection and luciferase assay

After the cell confluence to 80%-90%, we transfected miR-146a mimics (Sangon Biotech, Shanghai, China) using Lipofectamine 2000 (Invitrogen, Carlsbad, CA, USA) following manufacturer's instruction. RAW 267.4 transfected with Luciferase-labeled miR-640 mimics (15 ng) via adeno-associated virus (AAV) were isolated after undergoing 72 h transfection. Luciferase activity was detected using Luciferase assay system (Promega, Madison, WI, USA) directed by manufacturer's protocol.

2.3. Mice

C57/B6J male mice (six to eight-week-old, 20 g - 22 g) purchased. Mice were provided with available food and water and housed in cages with suitable temperature (22°C-24°C), humidity (55%-60%), and 12 h/12 h light/dark cycle.

2.4. Grouping and ALI Modeling

Mice were randomly divided into four groups: control group (CON, n=6); LPS modeling ALI group (LPS, n=6); miR-146a mimics control+LPS modeling ALI group (LPS+MMC CON, n=6); miR-146a mimics+ LPS modeling ALI group (LPS+MMC, n=6). For modeling, tail intravenous injections of miR-146a mimics control and miR-146a mimics were administered at 72 h before ALI induction. Next, 25 μg LPS dissolved in 75 μL phosphate-buffered saline (PBS) was treated in mice to establish the ALI model through transtracheal injection.

2.5. Quantitative Reverse Transcription-Polymerase Chain Reaction (qRT-PCR)

RNA was extracted from RAW 267.4 using TRIzol reagent (Invitrogen, Carlsbad, CA, USA) according to the manufacturer's protocols. Reverse transcription was conducted using PrimeScript™ RT Master Mix (Applied Biosystems, Foster City, CA, USA). Then, the procedure of qRT-PCR was conducted to quantify mRNA expression level using SYBR Green Master Mix (Applied Biosystems, Foster City, CA, USA). Glyceraldehyde 3-phosphate dehydrogenase (GAPDH) and U6 were used for normalization. Primer sequences are listed in Table 1.

2.6. Western Blot (WB) analysis

RAW 267.4 cells were harvested and extracted to protein using lysis buffer in Total Protein Extraction Kit (Keygen, Nanjing, China) according to the manufacturer's instructions. Proteins were measured with the Enhanced bicinchoninic acid (BCA) Protein Assay Kit (Beyotime, Shanghai, China) and balanced. After electrophoresis, transferring and blocking, proteins were incubated overnight with anti-Notch 1 (Abcam, Cambridge, MA, USA, 1:1000) and anti-GAPDH (Cell Signaling Technology, Danvers, MA, USA, 1:1000). Washing with Tris-Buffered Saline and Tween-20 (TBST), the membrane was incubated with secondary antibody (Proteintech, Wuhan, China, 1:10000) for 1 h at room temperature. Proteins were visualized and detected using an enhanced chemiluminescence (ECL) system.

2.7. Histologic staining

Lung tissues were fixated with 4% paraformaldehyde and conducted dehydration using different gradient alcohols. Then, samples were embedded into paraffin and cut into sections (5 μm). Hematoxylin-eosin staining was conducted using Hematoxylin and Eosin Staining Kit (Beyotime, Shanghai, China).

2.8. Immumohistochemical (IHC) staining

Hepatic tissue was obtained through fixation and dehy-

Table 1. Primer sequences of quantitative reverse transcription-polymerase chain reaction.

Oligo Name		Sequence (5' --------> 3')
miR-146a	Forward	GAACTGAATTCCATGGGTTGTGT
	Reverse	GCCCACGATGACAGAGAGATCC
GAPDH	Forward	GTCTTCACCACCATGGAG
	Reverse	CCAAAGTTGTCATGGATGACC
Arg1	Forward	TCATGGAAGTGAACCCAACTCTTG
	Reverse	TCAGTCCCTGGCTTATGGTTACC
Notch1	Forward	CCAGCATGGCCAGCTCTGG
	Reverse	CATCCAGATCTGTGGCCCTGTT
iNOS	Forward	GTTCTCAGCCCAACAATACAAGA
	Reverse	GTGGACGGGTCGATGTCAC
U6	Forward	GTAGATACTGCAGTACG
	Reverse	ATCGCATGACGTACCTGAGC

dration, then it was embedded into paraffin and cut into sections. Following deparaffinization and rehydration, tissue section was conducted immunohistochemistry (IHC) with iNOS (Abcam, Cambridge, MA, USA, 1:100) and Arg1 (Abcam, Cambridge, MA, USA, 1:200). Then, images were visualized using a microscope.

2.9. Enzyme Linked Immunosorbent Assay (ELISA)

Serum was taken from mice by ophthalmectomy. The medium and serum were centrifuged for 10 min and then the supernatant was collected, respectively. Standard product was added to a 96-well plate with different concentrations. Then, the ELISA was performed using ELISA Kits (Beyotime, Shanghai, China). The absorbance (OD value) of each sample was measured at 450 nm using a spectrophotometer.

2.10. Statistical analysis

Data were displayed as the means ± standard deviations (SD). Comparison in two groups was analyzed using Student's t-test and comparison in multiple groups was calculated using One-way analysis of variance (ANOVA) test followed by Post-Hoc Test (Least Significant Difference). Data were assessed using GraphPad Prism 6.0 (La Jolla, CA, USA). Value $P<0.05$ was considered as statistical significance.

3. Results

3.1. The difference of miR-146a expression with Notch 1 pathway change in vitro and vivo

First, we explored whether miR-146a expression alters in LPS or IL-4-induced RAW 267.4 cells. RNA was extracted to detect miR-146a levels in type M1 and M2 cell. The result showed that miR-146a expression decreased in LPS-induced M1 cells, however, the level of miR-146a exhibited a marked elevation in IL-4-induced M2 cell (Figure 1A-1B). Then, the RNA level of miR-146a was measured in ALI lung tissue at 24 hours post-injury, finding that miR-146a expression decreased at post-ALI (Figure 1C). Notch 1 pathway has been demonstrated to play a critical role in macrophage polarization. Hence, to verify whether miR-146a targets Notch 1 pathway to influence the direction of cell polarization, we utilized miR-146a mimics and miR-146a mimics control in LPS-induced RAW 267.4 cell and detected transfection level and Notch 1 pathway expression, suggesting that miR-146a mimics overexpressed miR-146a level and miR-146a mimics control did not affect miR-146a, Notch 1 pathway significantly increased after LPS treatment but miR-146a increase inhibited Notch 1 pathway expression (Figure 1D-1E). Moreover, luciferase report exhibited that miR-640 mimics down-regulated Notch 1 level in macrophage (Figure 1F). Therefore, the above results indicate that miR-146a influences macrophage polarization targeting Notch 1 pathway and may regulate ALI progression.

3.2. Overexpression of miR-146a inhibits inflammation by regulating cell polarization

Furtherly, we explored whether miR-146a overexpression affects macrophage inflammation levels with LPS administration. QRT-PCR displayed that the inducible nitric oxide synthase (iNOS) remarkably decreased following miR-146a mimics treatment, but arginase-1 (Arg1) was up-regulated after miR-146a increase (Figure 2A-2B), indicating increased miR-146a mediates the phenotype of macrophage to M2 polarization. Besides, ELISA on a variety of pro-inflammatory factors, tumor necrosis factor-alpha (TNF-α) and interleukin 1 beta (IL-1β), and anti-inflammatory interleukin 10 (IL-10) in supernatant medium showed that the overexpression of miR-146a decreased the expression of TNF-α and IL-1β, while IL-10 level remarkably increased following miR-146a mimics employment (Figure 2C-2E). To understand the effect of miR-146a on the expression of Notch 1 in macrophage, we visualized the expression of Notch 1 by western blotting, and found that the expression of Notch 1 following mimics treatment was significantly reduced (Figure 2F). So, the results show that miR-146a increases mitigates inflammation and regu-

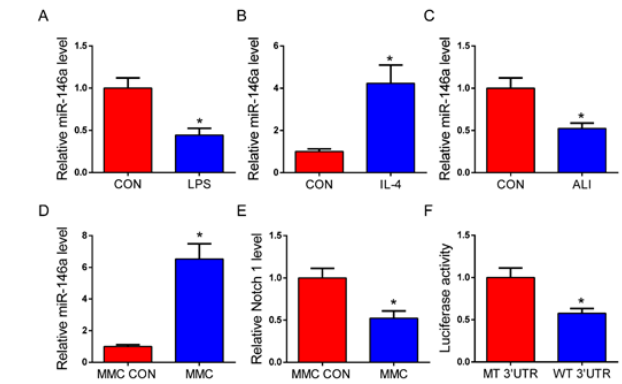

Fig. 1. The difference of miR-146a expression with Notch 1 pathway change *in vitro* and *in vivo*. (A) Representative miR-146a level in RAW 267.4 cell at 24 h post-LPS stimuli. (B) Representative miR-146a level in RAW 267.4 cells at 24 h post IL-4 stimuli. (C) Representative miR-146a level in mice lung tissue at 24 h post ALI. "*" means vs. CON group with statistical significance. (D) Representative miR-146a level in RAW 267.4 cell with MMC CON and MMC treatment at 24 h post-LPS stimuli. (E) Representative Notch 1 RNA level in RAW 267.4 cell with MMC CON and MMC treatment at 24 h post-LPS stimuli. "*" means vs. MMC CON group with statistical significance. (F) Representative luciferase activity of Notch 1 MT-3'UTR and WT-3'UTR. "*" means *vs.* MT-3'UTR group with statistical significance.

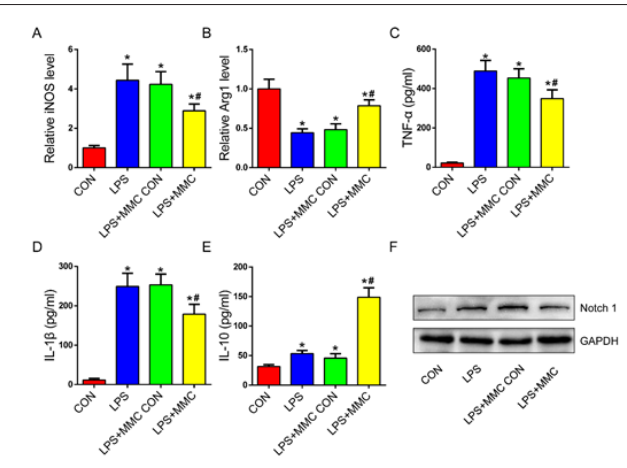

Fig. 2. Overexpression of miR-146a inhibits inflammation by regulation of cell polarization. (A-B) The representative RNA level of iNOS and Arg1 in CON, LPS, LPS+MMC CON and LPS+MMC group. (C-E) Representative ELISA of TNF-α, IL-1β and IL-10 in CON, LPS, LPS+MMC CON and LPS+MMC group. (F) Representative Western blotting of Notch 1 in CON, LPS, LPS+MMC CON and LPS+MMC group. "*" means *vs.* CON group with statistical significance. "#" means *vs.* LPS+MMC CON group with statistical significance.

lates cell phenotype by down-regulating Notch 1 pathway.

3.3. MiR-146a increase alleviates LPS-induced inflammation in ALI mice

We evaluated the therapeutic effect of miR-146a overexpression on ALI in mice and achieved excessive miR-146a expression through transfection with miR-146a mimics. ELISA in BALF showed that the protein level of TNF-α and IL-1β decreased following miR-146a mimics transfection, while the protein level of IL-10 increased significantly after overexpression of miR-146a (Figure 3A-3C). Immunohistochemistry showed that iNOS positive region in tissue reduced significantly after miR-146a overexpression administration, but the expression of Arg1 in tissue increased significantly with miR-146a mimics (Figure 3D). Therefore, the above results suggest that miR-146a increase decreased inflammation levels in ALI mice.

3.4. Increased miR-146a protects capillary barrier and pulmonary histology in ALI

We examined the treatment of miR-146a overexpression on capillary barrier and hepatic histology and function following ALI. Evans blue assay displayed a severely dyed tissue after LPS utilization, while miR-146a alleviated transudatory dye in lung tissue in ALI mice (Figure 4A). Besides, we weighed the wet/dry weight of lung tissue, it was found that miR-146a treatment markedly reduced the ratio of wet/dry weight in ALI mice lung (Figure 4B), indicating increased miR-146a potentially improved the alveolar-capillary barrier during the inflammation stage. From a histological aspect, HE staining showed LPS-induced excessive macrophages and neutrophils accumulating in interstitial and alveolar spaces as well as thickened alveolar walls associated with hemorrhage, however, miR-146a treatment alleviated these pathological phenomena in lung tissue (Figure 4C). Therefore, miR-146a overexpression ameliorates lung histology in ALI.

4. Discussion

ALI is a process of inflammatory development, which can produce many cytokines. However, numerous miRNAs play a causal regulatory role in inflammatory progress [18,19]. A previous study has suggested that miR-146a served as an inflammation-associated microRNA in human temporal lobe epilepsy [20] and Feng et al. [21] reported that miR-146a mediates inflammatory changes in the heart in diabetes. Consistently, we here demonstrated that miR-146a, as an inflammatory resister, was inhibited in the LPS induced vitro type M1 macrophage and vivo ALI model. However, we witnessed miR-146a increase in type M2 macrophage. A study reported by Song et al. [22] consistently showed enhanced therapeutic efficacy of exosomal miR-146a in sepsis. Hence, we hypothesized that overexpression of miR-146a in ALI through regulating macrophage polarization may play a protective role in improving damage effects during inflammation. Guan et al. [23] proved that increased miR-146a attenuated aging- and trauma-induced osteoarthritis *via* inhibiting Notch 1 and pro-inflammatory cytokines-mediated catabolism. Moreover, evidence showed the regulation of macrophage polarization *via* miR-146a/ Notch 1 [24]. Therefore, we measured the correlation between miR-146a and Notch 1 pathway level in RAW 267.4 cell line *via* LPS stimulation. Consistent with the earlier researches, we found that increased expression of miR-146a significantly inhibited Notch 1 level in RAW 267.4 cells. To further verify the miR-146a/ Notch 1 axis, we overexpressed miR-146a in ALI mice and found that miR-146a consistently decreased Notch 1 expression *in vivo*. Besides, the inflammatory cytokines in macrophage and BALF by LPS induction exhibited a distinct decrease after miR-146a overexpression. Oppositely, the classical anti-inflammatory cytokine IL-10 prominently increased in both of vitro macrophage and vivo ALI model with increased miR-146a. Multiple studies [25,26] suggest that iNOS displays as a biomarker in type M1 macrophages and Arg1 as a type M2 marker. In the present study, we evaluated the level of macrophage polarization *via* examining iNOS and Arg1 expression *in vitro* and *in vivo*. We proved lower RNA expression of iNOS and higher RNA expression of Arg1 in macrophages after miR-146a mimics treatment. In ALI mice, miR-146a increase likewise attenuated iNOS positive region but elevated Arg1 positive region in lung tissue, further indicating that overexpression of miR-146a modulated macrophage differentiation *via* suppression of Notch 1 pathway. It has been certified that a band of pathological cascades associated with inflammation, such as oxidative stress and

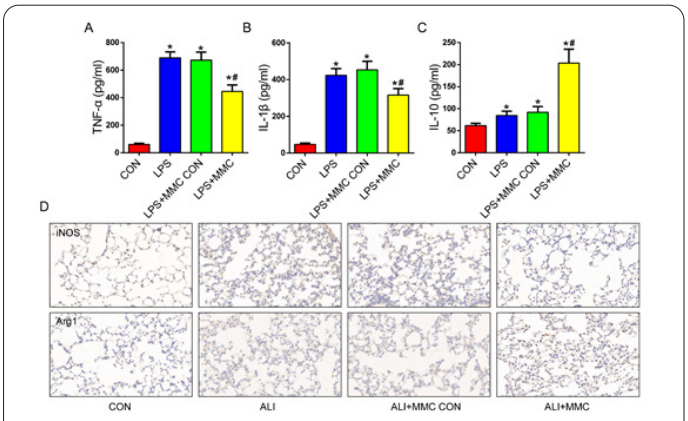

Fig. 3. MiR-146a increase alleviates LPS-induced inflammation in ALI mice. (A-C) Representative ELISA of TNF-α, IL-1β and IL-10 in BALF in CON, LPS, LPS+MMC CON and LPS+MMC group. "*" means vs. CON group with statistical significance. "#" means vs. LPS+MMC CON group with statistical significance. (D) Representative IHC of iNOS and Arg1 in CON, LPS, LPS+MMC CON and LPS+MMC group (magnification: 100×).

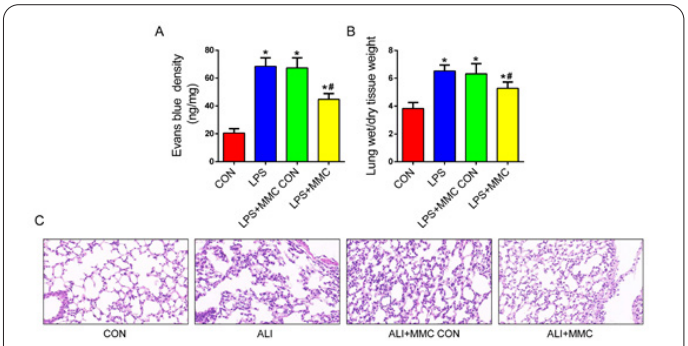

Fig. 4. Increased miR-146a protects capillary barrier and pulmonary histology in ALI. (A) Representative Evans blue lung tissue in CON, LPS, LPS+MMC CON and LPS+MMC group. (B) Representative ratio of lung wet/dry weight in CON, LPS, LPS+MMC CON and LPS+MMC group. "*" means *vs.* CON group with statistical significance. "#" means *vs.* LPS+MMC CON group with statistical significance. (C) Representative HE staining of lung tissue in CON, LPS, LPS+MMC CON and LPS+MMC group (magnification: 100×).

apoptosis, destroy the integrity of alveoli capillary barrier and pulmonary tissue. We herein witnessed that LPS-induced ALI severely damages alveolar-capillary barrier and contributed to extensive Evans blue dye in lung tissue. However, the Evans blue lung tissues using mimics administration remarkably decreased. Hence, the degree of edema reflected on wet/dry weight of lung tissue was mitigated, illustrating that increased miR-146a treatment might improve alveoli capillary barrier owing to the alleviated inflammation and potential repair capacity of type M2 cells. The HE staining from histology showed fewer infiltrative macrophages and neutrophil and ameliorative alveolar walls in lung tissue with miR-146a mimics administration. The result further indicated that miR-146a overexpression corrected inflammation and edema in ALI mice. Evidences exhibit that overexpression of miR-146a inhibits the apoptosis in rat hippocampal neurons [27] and in primary human retinal microvascular endothelial cells [28]. However, few studies suggested miR-146a induced apoptosis in neuroblastoma cells and inhibited proliferation [29] and induced apoptosis in osteoblast [30-33]. Further studies are needed to illuminate miR-146a regulated mechanism to apoptosis in ALI. Gathering the results, we verify that miR-146a increase leads to type M2 macrophage polarization, mitigates inflammation and attenuates leukocyte infiltration, tissue edema, and destruction of the alveolar-capillary barrier during ALI. Therefore, miR-146a is a promising therapeutic target that alleviates ALI and complements the previously reported studies concerning miRNAs and ALI. Whereas, further investigation concerning other pathophysiological regulation and pulmonary diseases needs to be a critical part of miR-146a treatment.

5. Conclusions

These results indicate that miR-146a induces an-inflammatory differentiation of macrophage *via* restraining Notch 1 signaling pathway. Hence, increasing miR-146a ameliorates ALI by preventing macrophage-induced inflammation. MiR-146a overexpression may become a novel therapy aspect for ALI in the future.

Conflict of interests

The author has no conflicts with any step of the article preparation.

Consent for publications

The author read and approved the final manuscript for publication.

Ethics approval and consent to participate

This study was approved by the Animal Ethics Committee of Nantong University Animal Center.

Informed consent

The authors declare not used any patients in this research.

Availability of data and material

The data that support the findings of this study are available from the corresponding author upon reasonable request

Authors' contributions

QZ, YW: Conceptualization, methodology, writing original draft preparation. JZ, RK: Investigation, software, statistical analysis. SJ: Reviewing and editing, funding acquisition, supervision. All authors read and approved the final manuscript.

Funding

This study was supported by Changzhou green seedling talent project (project No.CZQM2022021).

References

1. Yu C, Qichang L, Zhimin Z, Zhongqiang T, Yanrui W, Haiyan X (2023) Value of plasma AGEs and sRAGE expression in predicting the occurrence of ARDS in elderly COPD patients. Cell Mol Biol 69:135-138. doi: 10.14715/cmb/2023.69.3.19
2. Matthay MA, Ware LB, Zimmerman GA (2012) The acute respiratory distress syndrome. J Clin Invest 122:2731-2740. doi: 10.1172/JCI60331
3. Wheeler AP, Bernard GR (2007) Acute lung injury and the acute respiratory distress syndrome: a clinical review. Lancet 369:1553-1564. doi: 10.1016/S0140-6736(07)60604-7
4. Zhang Y, Zhang J, Wang M, Zhao T (2022) Repairing Effect of New Dexamethasone Nanoparticles in the Treatment of Acute Lung Injury and Cluster Nursing. Cell Mol Biol 68:140-148. doi: 10.14715/cmb/2022.68.3.17
5. Rainer TH, Lam PK, Wong EM, Cocks RA (1999) Derivation of a prediction rule for post-traumatic acute lung injury. Resuscitation 42:187-196. doi: 10.1016/s0300-9572(99)00089-1
6. Wang L, Yuan R, Yao C, Wu Q, Christelle M, Xie W et al (2014) Effects of resolvin D1 on inflammatory responses and oxidative stress of lipopolysaccharide-induced acute lung injury in mice. Chin Med J 127:803-809.
7. Du X, Feng W, Zhang S, Lin X, Song L, Shen N et al (2023) Salidroside attenuates LPS-induced inflammatory activation in young rats with acute lung injury via PI3K/Akt signaling pathway. Cell Mol Biol 69:124-128. doi: 10.14715/cmb/2023.69.3.17
8. Liu D, Dong Y, Liu Z, Niu B, Wang Y, Gao X (2014) Impact of TREM-2 gene silencing on inflammatory response of endotoxin-induced acute lung injury in mice. Mol Cell Biochem 394:155-161. doi: 10.1007/s11010-014-2091-6
9. Neudecker V, Brodsky KS, Clambey ET, Schmidt EP, Packard TA, Davenport B et al (2017) Neutrophil transfer of miR-223 to lung epithelial cells dampens acute lung injury in mice. Sci Transl Med 9:eaah5360. doi: 10.1126/scitranslmed.aah5360
10. Dong W, He B, Qian H, Liu Q, Wang D, Li J et al (2018) RAB26-dependent autophagy protects adherens junctional integrity in acute lung injury. Autophagy 14:1677-1692. doi: 10.1080/15548627.2018.1476811
11. Hu Y, Lou J, Mao YY, Lai TW, Liu LY, Zhu C et al (2016) Activation of MTOR in pulmonary epithelium promotes LPS-induced acute lung injury. Autophagy 12:2286-2299. doi: 10.1080/15548627.2016.1230584
12. Li J, Tan S, Kooger R, Zhang C, Zhang Y (2014) MicroRNAs as novel biological targets for detection and regulation. Chem Soc Rev 43:506-517. doi: 10.1039/c3cs60312a
13. Ambros V (2013) Victor Ambros: the broad scope of microRNAs. Interview by Caitlin Sedwick. J Cell Biol 201:492-493. doi: 10.1083/jcb.2014pi
14. Gebert L, MacRae IJ (2019) Regulation of microRNA function in animals. Nat Rev Mol Cell Biol 20:21-37. doi: 10.1038/s41580-018-0045-7
15. He K, Sun Y, Xiao H, Ge C, Li F, Han Z (2017) Multiple miRNAs jointly regulate the biosynthesis of ecdysteroid in the holometabolous insects, Chilo suppressalis. Rna 23:1817-1833. doi: 10.1261/rna.061408.117

16. Feng Z, Qi S, Zhang Y, Qi Z, Yan L, Zhou J et al (2017) Ly6G+ neutrophil-derived miR-223 inhibits the NLRP3 inflammasome in mitochondrial DAMP-induced acute lung injury. Cell Death Dis 8:e3170. doi: 10.1038/cddis.2017.549
17. Ying Y, Mao Y, Yao M (2019) NLRP3 Inflammasome Activation by MicroRNA-495 Promoter Methylation May Contribute to the Progression of Acute Lung Injury. Mol Ther Nucleic Acids 18:801-814. doi: 10.1016/j.omtn.2019.08.028
18. Tili E, Michaille JJ, Croce CM (2013) MicroRNAs play a central role in molecular dysfunctions linking inflammation with cancer. Immunol Rev 253:167-184. doi: 10.1111/imr.12050
19. Rebane A, Akdis CA (2013) MicroRNAs: Essential players in the regulation of inflammation. J Allergy Clin Immunol 132:15-26. doi: 10.1016/j.jaci.2013.04.011
20. Li TR, Jia YJ, Ma C, Qiu WY, Wang Q, Shao XQ et al (2018) The role of the microRNA-146a/complement factor H/interleukin-1beta-mediated inflammatory loop circuit in the perpetuate inflammation of chronic temporal lobe epilepsy. Dis Model Mech 11:dmm031708. doi: 10.1242/dmm.031708
21. Feng B, Chen S, Gordon AD, Chakrabarti S (2017) miR-146a mediates inflammatory changes and fibrosis in the heart in diabetes. J Mol Cell Cardiol 105:70-76. doi: 10.1016/j.yjmcc.2017.03.002
22. Song Y, Dou H, Li X, Zhao X, Li Y, Liu D et al (2017) Exosomal miR-146a Contributes to the Enhanced Therapeutic Efficacy of Interleukin-1beta-Primed Mesenchymal Stem Cells Against Sepsis. Stem Cells 35:1208-1221. doi: 10.1002/stem.2564
23. Guan YJ, Li J, Yang X, Du S, Ding J, Gao Y et al (2018) Evidence that miR-146a attenuates aging- and trauma-induced osteoarthritis by inhibiting Notch1, IL-6, and IL-1 mediated catabolism. Aging Cell 17:e12752. doi: 10.1111/acel.12752
24. Huang C, Liu XJ, QunZhou, Xie J, Ma TT, Meng XM et al (2016) MiR-146a modulates macrophage polarization by inhibiting Notch1 pathway in RAW264.7 macrophages. Int Immunopharmacol 32:46-54. doi: 10.1016/j.intimp.2016.01.009
25. Garg K, Pullen NA, Oskeritzian CA, Ryan JJ, Bowlin GL (2013) Macrophage functional polarization (M1/M2) in response to varying fiber and pore dimensions of electrospun scaffolds. Biomaterials 34:4439-4451. doi: 10.1016/j.biomaterials.2013.02.065
26. Edin S, Wikberg ML, Dahlin AM, Rutegard J, Oberg A, Oldenborg PA et al (2012) The distribution of macrophages with a M1 or M2 phenotype in relation to prognosis and the molecular characteristics of colorectal cancer. Plos One 7:e47045. doi: 10.1371/journal.pone.0047045
27. Huan S, Jin J, Shi CX, Li T, Dai Z, Fu XJ (2020) Overexpression of miR-146a inhibits the apoptosis of hippocampal neurons of rats with cerebral hemorrhage by regulating autophagy. Hum Exp Toxicol 39:1178-1189. doi: 10.1177/0960327120907131
28. Ye EA, Steinle JJ (2017) miR-146a suppresses STAT3/VEGF pathways and reduces apoptosis through IL-6 signaling in primary human retinal microvascular endothelial cells in high glucose conditions. Vision Res 139:15-22. doi: 10.1016/j.visres.2017.03.009
29. Li SH, Li JP, Chen L, Liu JL (2018) miR-146a induces apoptosis in neuroblastoma cells by targeting BCL11A. Med Hypotheses 117:21-27. doi: 10.1016/j.mehy.2018.05.019
30. Azizi Dargahlou S, Iriti M, Pouresmaeil M, Goh LPW. (2023) MicroRNAs; their therapeutic and biomarker properties. Cell Mol Biomed Rep 3(2): 73-88. doi: 10.55705/cmbr.2022.365396.1085
31. Kanwal N, Al Samarrai O, Al-Zaidi HMH, Mirzaei A, Heidari M. (2023). Comprehensive analysis of microRNA (miRNA) in cancer cells. Cell Mol Biomed Rep 3(2): 89-97. doi: 10.55705/cmbr.2022.364591.1070.
32. Sasani S, Rashidi Monfared S, Mirzaei AR (2024). Identification of some Echinophora platyloba miRNAs using computational methods and the effect of these miRNAs in the expression of TLN2 and ZNF521 genes in different human body organs. Cell Mol Biomed Rep 4(1): 43-53. doi: 10.55705/cmbr.2023.386145.1100.
33. Zhang B, Yi J, Zhang CL, Zhang QH, Xu JF, Shen HQ et al (2017) MiR-146a inhibits proliferation and induces apoptosis in murine osteoblastic MC3T3-E1 by regulating Bcl2. Eur Rev Med Pharmacol Sci 21:3754-3762.